Vortical motions driven by supernova explosions

By MAARIT J. KORPI[1], AXEL BRANDENBURG[2], ANVAR SHUKUROV[2] AND ILKKA TUOMINEN[1]

[1]Astronomy Division, University of Oulu, P.O. Box 333, 90571 Oulu, Finland

[2]Department of Mathematics, University of Newcastle upon Tyne, NE1 7RU, UK

We investigate the generation of vorticity in supernova driven interstellar turbulence using a local three-dimensional MHD model. Our model includes the effects of density stratification, compressibility, magnetic fields, large-scale shear due to galactic differential rotation, heating via supernova explosions and parameterized radiative cooling of the interstellar medium; we also include viscosity and resistivity. We allow for multiple supernovae, which are distributed randomly in the galactic disc and exponentially in the vertical direction. When supernovae are infrequent, so that there is no interactions between supernova remnants, the dynamics of the system is dominated by strong shocks driven by the young remnants. Supernova interactions, where shock fronts from younger remnants encounter the dense shells of the older remnants, were found to produce vorticity via the baroclinic effect. Vorticity generated by the baroclinic effect was observed to be amplified by the stretching of vortex lines, these two vorticity production mechanisms being of equal importance after 1.5×10^8 years. Motions driven by the supernova explosions also amplify the magnetic field via stretching and compression. This generates a random component from a uniform azimuthal magnetic field prescribed as an initial condition and maintains it against Ohmic losses.

1. Introduction

The interstellar medium (ISM) is in a state of a compressible, inhomogeneous and anisotropic turbulent flow. There are several energy sources for the interstellar turbulence. Stellar winds, supernova (SN) explosions and superbubbles heat, accelerate and compress the ISM driving shock waves (e.g. Ostriker & McKee 1988). Other possible sources of interstellar turbulence include the Parker instability (Parker 1992), the Balbus–Hawley instability (Balbus & Hawley 1991) and large scale shear stresses due to galactic differential rotation (Fleck 1981). It is believed, however, that SN explosions are a dominant source of the turbulent energy at scales of the order of 10–100 pc.

The energy released by SNe is converted into kinetic energy of turbulence in the ISM at late stages of the evolution of an SN remnant when the expansion velocity becomes comparable to the sound speed in the ambient medium, $c_{\rm s} \simeq 10\,{\rm km\,s^{-1}}$. The driving force is potential, but the observed spectrum of interstellar turbulence is close to that of Kolmogorov turbulence (Armstrong *et al.* 1981; Armstrong *et al.* 1995), so the motions are presumed to have significant vorticity.

Possible mechanisms of vorticity generation were recently reviewed by Chernin (1996). Our model allows detailed study of different mechanisms of vorticity generation, but we focus our attention on the baroclinic effect and stretching of vortex lines by the random velocity field produced by SN explosions.

2. The model

We investigate supernova driven interstellar turbulence using a local three-dimensional, non-ideal MHD model, which includes the effects of density stratification in the galactic

gravity field, compressibility, magnetic fields, heating via supernova explosions, radiative cooling of the ISM and large scale shear due to galactic differential rotation. We adopt a local Cartesian frame of reference, which rotates on a circular orbit with radius R and angular velocity Ω_0 about the galactic centre, with x, y and z corresponding to the radial, azimuthal and vertical directions, respectively. Under the local approximation the shear due to galactic differential rotation translates to a linear shear velocity $U = -q\Omega_0 x$ (Wisdom & Tremaine 1988), where $q = -\partial \ln \Omega / \partial \ln r$ is the shear parameter, $q = 1$ for a flat rotation curve, $\Omega \propto r^{-1}$. In the following we solve for deviations $\mathbf{u}$ from this basic flow. We solve the standard non-ideal MHD equations, namely the uncurled induction equation for the magnetic vector potential, the momentum equation, the energy equation and the continuity equation. Supernova heating and radiative cooling are modelled by source and loss terms in the energy equation.

Supernovae are modelled as instantaneous explosive events releasing thermal energy. The energy is fed into the system via a localized heating term (per unit mass) of the form

$$\Gamma = \xi(\mathbf{r}, t)\, E_{\rm SN} / (\rho V) \,, \tag{2.1}$$

where $\xi(\mathbf{r}, t)$ is a random function ($\xi = 1$ in a small volume V during an energy release event and zero otherwise), $E_{\rm SN}$ is the explosion energy of a single event, ρ is density at the explosion site and V is the volume where the SN energy is released; $\xi(t)$ is set to be one during only one timestep, which is typically 10–100 years. In the vertical direction we assume exponential distribution of SNe with scale height $H_{\rm SN}$ yielding explosion rate per unit volume

$$\sigma(z) = \frac{\sigma_0}{2H_{\rm SN}} \exp\left(-\left|z\right| / H_{\rm SN}\right) \,, \tag{2.2}$$

where σ_0 is the explosion rate per unit area. Supernova heating is balanced by radiative cooling. The cooling function is adopted from Vázquez-Semadeni *et al.* (1996. Since we do not include consistently all heating sources in the ISM, we use a correction factor C (< 1), which is selected to reach a precise long-term balance of heating and cooling. The cooling function adopted does not allow any thermally unstable phases at $T < 10^5$ K.

Our equations are solved numerically using a third-order Hyman scheme (Hyman 1979) for the time stepping and sixth-order compact scheme for the spatial derivatives (Lele, 1992). We adopt artificial viscosities and fluxes to stabilize advection and waves. The boundary conditions adopted are periodic in the azimuthal (y) direction, stress free and electrically insulating in the vertical (z) direction, and in the radial (x) direction periodic boundary conditions at sliding boundaries allow for the effects of the shear flow. A more detailed description of the code is given in Brandenburg *et al.* (1995); see also Nordlund & Stein (1990).

Our model is broadly similar to that of Vázquez-Semadeni *et al.* (1996 and references therein) who consider two-dimensional models of turbulence driven by stellar winds in denser phases of the ISM. However, in order to avoid complications associated with dense clouds resulting from thermal instability, we concentrate on the rarefied phases, namely the warm and hot diffuse components of the ISM. Our heating and turbulence are produced by vigorous explosive events rather than by prolonged energy injection from stellar winds.

2.1. *Parameters*

We take a box of dimensions $L_x = L_y = 0.5$ kpc and $L_z = 1.0$ kpc located at reference radius R=10 kpc in the Galaxy. We have performed both low ($21 \times 21 \times 42$) and high resolution ($81 \times 81 \times 162$) calculations with the mesh sizes $\delta x = \delta y = \delta z = 25$ pc and

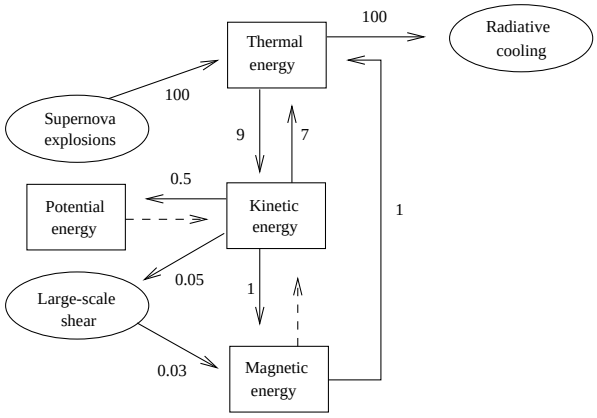

FIGURE 1. The energy balance in the simulations. Square boxes show energy reservoirs, and ellipses indicate sources and sinks of energy. Arrows indicate dominant routes of energy transformations in our model with numbers giving the percentage of the total energy transferred in 2×10^8 years, 5×10^{54} erg kpc^{-3}. Dashed lines indicate other possible directions of energy flow which, however, are not well pronounced in our simulations.

$\delta x = \delta y = \delta z = 6$ pc, respectively. We adopt an angular velocity representative of the solar neighbourhood $\Omega_0 = 25$ km s^{-1} kpc^{-1}. Our initial state represents a quiescent warm interstellar medium (we recall that the thermal instability is suppressed). We have initially uniform internal energy $e = e_0$, which is determined by the initial isothermal sound speed $c_{s0} = 10\,\mathrm{km\,s^{-1}}$ corresponding to $T \approx 10^4$ K. In the initial state we adopt hydrostatic equilibrium with

$$\rho = \rho_0 \exp\left[1 - \left(1 + z^2/H^2\right)^{1/2}\right] ,$$

where H=100 pc is the initial scale height of the disk and $\rho_0 = 0.1\,\mathrm{cm^{-3}}$ is the density at the galactic midplane. Initially we assume that $\mathbf{u} = 0$. We start with a large scale azimuthal magnetic field $\mathbf{B} \propto (0, \sin \pi z/L_z, 0)$, so the initial Alfvén speed is $10\,\mathrm{km\,s^{-1}}$.

For the parameters describing supernova explosions we take $E_{\rm SN} = 10^{51}$ erg, $H_{\rm SN}$ =265 pc and $\sigma_0 = 1.9 \times 10^{-5}$ kpc^{-2} yr^{-1} describing Type II SNe. These values give approximately one supernova in 2×10^5 years at the galactic midplane. The time steps in the simulations were typically 10^3 and 10^4 years in the high- and low-resolution runs, respectively.

3. Results

3.1. *Energy balance*

We show in Fig.1 the energy balance in our simulations. The only major source of energy are SN explosions which inject thermal energy. About 9% of the thermal energy released by SN explosions is converted into kinetic energy of the ISM. This figure agrees well with detailed simulations of the evolution of SN remnants (see, e.g., Chevalier 1977, Lozinskaya 1992), and we consider this as important evidence that our implementation of SN explosions is realistic and adequate even in low resolution runs.

The effects associated with large-scale (rotational) shear are minor because our runs last for only one rotation period or less. However, we anticipate that the long-term

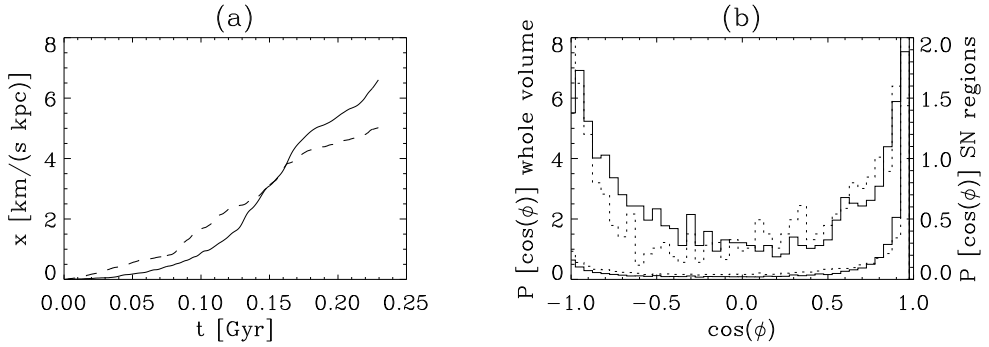

FIGURE 2. (a): The vorticity production averaged over the computation volume (in $\mathrm{km\,s^{-1}\,kpc^{-1}}$) due to vortex line stretching (solid) and the baroclinic term (dashed) as functions of time. (b): The probability density for $\cos\phi$ with ϕ the angle between temperature and entropy gradients. The two lower curves (with the scale on the left y-axis) are obtained by averaging over the whole computational volume at the final stage (dotted) and at the initial stage of vorticity growth (solid). The two upper curves (with the scale on the right y-axis) are obtained by averaging over a thinner layer (about 1/4 of the total vertical extent) near the midplane where the number density of SNe is maximum at the final stage (dotted) and at the initial stage of vorticity growth (solid).

importance of differential rotation is more significant, especially for the evolution of the large-scale magnetic field.

About 15% of the kinetic energy available is converted into magnetic energy. This is enough to maintain the magnetic field; we stress that we only adopt a large scale azimuthal (y) magnetic field initially, but it is *not* imposed via boundary conditions, so it is free to decay. Instead, the azimuthal field remains strong during all the runs without any signs of decay. Moreover, the x and z components of the magnetic field, absent at the beginning of any run, grow rapidly when motions in the ISM develop. Magnetic fields generated and maintained in our model will be discussed elsewhere.

At early stages of the evolution, the system relaxes to a global steady state via oscillations in which the scale height of the gas varies at a period of 3×10^7 years, which is about three times the sound crossing time, H/c_{s0}. These oscillations dominate the exchange of energy between the potential and kinetic energy reservoirs; see Fig.1.

3.2. *Vorticity generation*

Although the forcing by SN explosions is a potential one, the motions in the diffuse gas quickly become vortical. The time dependencies of two relevant terms in the vorticity equation, the vortex stretching term and the baroclinic term, are shown in Fig.2(a). It can be easily seen that the baroclinic term is larger at early times. The vorticity stretching term, however, becomes comparable to and even exceeds the baroclinic term at later times. In general, the two terms are comparable and equally important. To verify the relevance of the baroclinic term we have plotted in Fig.2(b) the probability distribution function of the angle between the temperature and entropy gradients for different regions and stages of evolution. The tendency for the gradients to be inclined is stronger in the region where the SN number density is larger. This implies that the baroclinic term is most important near the shock fronts.

In conclusion, we have shown that SN driven turbulence is capable of producing significant amounts of vorticity, initially via the baroclinic term and at later times via the vortex stretching term. This appears to be different in previous simulations of explicitly

forced turbulence (Vázquez-Semadeni et al. 1996), where vortex stretching was found to act as a sink destroying potential vorticity. High resolution simulations with different parameters are now necessary to find out which of the results is robust. For example, are the exchange rates between different energy reservoirs representative for the Galaxy, or do they depend on resolution and the various parameters adopted? Also, in order to know whether or not dynamo action is at work we need to start with an initially weak magnetic field, to see whether there is a stage where the magnetic energy and the mean field increase exponentially in time.

This work was supported in part by the EC Human Capital and Mobility Networks project "Late type stars: activity, magnetism, turbulence" No. ERBCHRXCT940483 and a PPARC grant GR/L 30268. MJK acknowledges travel support from the University of Oulu.

REFERENCES

Armstrong, J. W., Cordes, J. M. and Rickett, B. J. 1981 Density power spectrum in the local interstellar medium *Nature* **291**, 561–564

Armstrong, J. Q., Rickett, B. J. and Spangler, S. R. 1995 Electron density power spectrum in the local interstellar medium *Astrophys. Journal* **443**: 209–221

Balbus, S. A. & Hawley, J. F. 1991 A powerful local shear instability in weakly magnetized disks. I - Linear analysis. II - Nonlinear evolution. *Astrophys. Journal* **376**, 214–233

Brandenburg, A., Nordlund, Å., Stein, R. F. and Torkelsson, U. 1995 Dynamo-generated turbulence and large-scale magnetic fields in a Keplerian shear flow. *Astrophys. Journal*, **446**, 741–754

Chernin, A.D. 1996 Shocks and vorticity in cosmic hydrodynamics *Vistas in Astronomy* **40**, 257–301

Chevalier, R.A. 1977 The interaction of supernovae with the interstellar medium *Ann. Rev. Astron. Astrophys.* **15**, 175–196

Fleck, R. C. 1981 On the generation and maintenance of turbulence in the interstellar medium *Astrophys. Journal* **246**, L151–L154

Hyman, J. M. 1979 A Method of Lines Approach to the Numerical Solution of Conservation Laws In: *Adv. of Computation Methods for Partial Differential Equations, Vol III*, Publ. IMACS (ed. R. Vichnevetsky & R. S. Stepleman), pp. 313-343

Lele, S. K. 1992 Compact finite difference schemes with spectral-like resolution. *J. Comput. Phys.* **103**, 16–42

Lozinskaya, T.A. 1992 *Supernovae and Stellar Wind in the Interstellar Medium,* American Institute of Physics, New York

Nordlund, Å. & Stein, R. F. 1990 3-D Simulations of Solar and Stellar Convection and Magnetoconvection *Comput. Phys. Commun.* **59**, 119–125

Ostriker, J. P. & McKee, C. F. 1988 Astrophysical blastwaves *Rev. Mod. Phys.* **60**, 1–68

Parker, E. N. 1992 Fast dynamos, cosmic rays and the galactic magnetic field *Astrophys. Journal* **401**, 634–663

Vázquez-Semadeni,E., Passot, T. and Pouquet, A. 1996 Influence of cooling-induced compressibility on the structure of turbulent flows and gravitational collapse. *Astrophys. Journal*, **473**, 881–893

Wisdom, J. and Tremaine, S. 1988 Local simulations of planetary rings. *Astron. Journal*, **95**, 925–940